Inorg. Chem. **2006**, *45*, 6179–6187

Control of Copper(I) Iodide Architectures by Ligand Design: Angular versus Linear Bridging Ligands

Frédéric Thébault, Sarah A. Barnett, Alexander J. Blake, Claire Wilson, Neil R. Champness,* and Martin Schröder*

School of Chemistry, The University of Nottingham, University Park, Nottingham NG7 2RD, U.K.

Received December 13, 2005

A family of coordination polymers formed by the reaction of copper(I) iodide with a range of angular bidentate or tridentate N-donor ligands is reported. The framework polymers $[CuI(dpt)]_\infty$ **1** [dpt = 2,4-bis(4-pyridyl)-1,3,5-triazine], $[CuI(dpb)]_\infty$ **2** [dpb = 1,4-bis-(4-pyridyl)-benzene], $[(CuI)_3(dpypy)_2]_\infty$ **3**, $[CuI(dpypy)]_\infty$ **4** [dpypy = 3,5-bis(4-pyridyl)-pyridine], and $[Cu_3I_3(pypm)]_\infty$ **5** [pypm = 5-(4-pyridyl)pyrimidine] have been prepared and structurally characterized. It was found that the angular nature of the dpypy and dpt ligands favors the formation of discrete $(CuI)_2$ dimeric subunits as observed in $[CuI(dpt)\cdot MeCN]_\infty$ **1** and $[(CuI)_3(dpypy)_2]_\infty$ **3**. In contrast, reaction with the linear ligand dpb affords $[CuI(dpb)]_\infty$ **2** which incorporates a one-dimensional $(CuI)_\infty$ chain structure. Moreover, the additional donor available on the central ring of the dpypy ligand generates a novel two-dimensional bilayer structure in **3**, in contrast to the one-dimensional ribbon structure observed in the case of **1**. Interestingly, the bilayer structure of **3** additionally exhibits 2-fold interpenetration. The reaction of CuI with dpypy produces not only **3** but a further product $[CuI(dpypy)]_\infty$ **4** that has been characterized as a one-dimensional chain constructed from trigonal-planar Cu(I) centers bridged by bidentate dpypy ligands. Compound **5**, $[Cu_3I_3(pypm)]_\infty$, exhibits a highly unusual three-dimensional structure in which the pypm ligand bridges two-dimensional brick-wall $(CuI)_\infty$ sheets.

Introduction

The construction of coordination frameworks is an extremely topical area of chemistry because of their potential as new materials with tunable properties.[1] As these materials become more highly evolved, properties can become more highly tuned, leading to the development of useful, functional, and even polyfunctional materials. The high levels of interest in this area of research arise also because the main synthetic methodology used in the construction of these materials, a building-block approach based upon bridging metal cationic nodes with bridging ligands, allows the potential for a high degree of design with targeting of specific properties.[2] However, the targeted synthesis of such polymers requires not only an appreciation of the variety of possible coordination framework materials that can be prepared from a given set of building-block components but also an appreciation of which structures and topologies are favored and why. The incorporation of building-blocks with a high degree of geometric flexibility can afford a large range of possible structures leading in turn to an almost complete absence of predictability.[3] However, this flexibility also can lead to the observation of highly unusual structures.[4]

For some time we have been interested in the large structural variation exhibited by copper(I) halides, pseudohalides [Cu(SCN)], and in particular copper(I) iodide[5–8] which are known to exhibit fluorescent properties.[9] The strongly coordinating nature of the halide anion is such that

* To whom correspondence should be addressed. E-mail: Neil.Champness@nottingham.ac.uk (N.R.C.), M.Schroder@nottingham.ac.uk (M.S.).

(1) (a) Noro, S.; Kitagawa, S.; Kondo, M.; Seki, K. *Angew. Chem., Int. Ed.* **2000**, *39*, 2082. (b) Kitaura, R.; Kitagawa, S.; Kubota, Y.; Kobayashi, T. C.; Kindo, K.; Mita, Y.; Matsuo, A.; Kobayashi, M.; Chang, H. C.; Ozawa, T. C.; Suzuki, M.; Sakata, M.; Takata, M. *Science* **2002**, *298*, 2358. (c) Kahn, O. *Acc. Chem. Res.* **2000**, *33*, 647. (d) Evans, O. R.; Lin, W. *Acc. Chem. Res.* **2002**, *35*, 511. (e) Maspoch, D.; Ruiz-Molina, D.; Wurst, K.; Domingo, N.; Cavallini, M.; Biscarini, F.; Tejada, J.; Rovira, C.; Veciana, J. *Nat. Mater.* **2003**, *2*, 190. (f) Coronado, E.; Galan-Mascaros, J. R.; Gomez-Garcia, C. J.; Laukhin, V. *Nature* **2000**, *408*, 447. (g) Champness, N. R.; Schröder, M. *Curr. Opin. Solid State Mater. Chem.* ***1998***, *3* 419.

(2) (a) Hoskins, B. F.; Robson, R. *J. Am. Chem. Soc.* **1990**, *112*, 1546. (b) Robson, R.; Abrahams, B. F.; Batten, S. R.; Gable, R. W.; Hoskins, B. F.; Liu, J. P. *ACS Symp. Ser.* **1992**, *499*, 256.

(3) (a) Barnett, S. A.; Champness, N. R. *Coord. Chem. Rev.* **2003**, *246*, 145. (b) Barnett, S. A.; Blake, A. J.; Champness, N. R.; Wilson, C. *J. Chem. Soc., Dalton Trans.* **2005**, 3852. (c) Oxtoby, N. S.; Blake, A. J.; Champness, N. R.; Wilson, C. *Proc. Natl. Acad. Sci. U.S.A.* **2002**, *99*, 4905.

10.1021/ic052130k CCC: $33.50
Published on Web 04/05/2006

it can bridge two or more copper centers giving neutral species of the form $(CuX)_n$ (X = Cl, Br or I; $n = 1, 2, 3, 4, ..., \infty$). These species can have discrete molecular structures (e.g. rhomboid dimer or cubane tetramers),[7a,10] one-dimensional structures (e.g. staircase chains, split staircase chains, zigzag chains, or hexagonal columns),[7b,c,11] or two-dimensional structures (e.g. corrugated sheets),[7c] which can be connected to form coordination polymers using diverse bridging ligands. For example, when combined with the bridging bidentate ligands pyrimidine, pyrazine, 4,4′-bipyridine, 2,7-diazapyrene, quinoxaline, and 4,7-phenanthroline, two-dimensional sheets comprising one-dimensional $(CuX)_\infty$ motifs linked by the bridging ligand are produced.[7b] Similarly, 1,3,5-triazine in combination with copper(I) halides generates three-dimensional arrays consisting of either one-dimensional $(CuX)_\infty$ motifs linked by tridentate triazine or two-dimensional $(CuX)_\infty$ motifs joined by bidentate triazine.[7c]

Chart 1

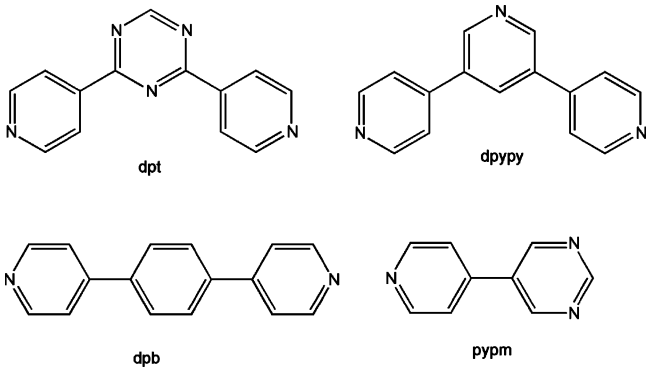

We report herein the synthesis, crystallization, and structural characterization of a range of CuI-based coordination polymer arrays formed using angular[12a,c] bidentate or tridentate N-donor ligands. The ligands (Chart 1) were chosen to illustrate the influence of the angular nature of the N-donor groups and to attempt to gain a degree of control over the nature of the $(CuI)_\infty$ motif adopted. As will be seen, the angular nature of the ligand, in the case of 3,5-bis(4-pyridyl)-pyridine (dpypy) and 2,4-bis(4-pyridyl)-1,3,5-triazine (dpt), can favor the formation of discrete $(CuI)_2$ dimeric subunits as observed in $[CuI(dpt)\cdot MeCN]_\infty$ **1** and $[(CuI)_3(dpypy)_2]_\infty$ **3** in preference to the one-dimensional $(CuI)_\infty$ chain structure seen for $[CuI(dpb)]_\infty$ **2** which contains the linear ligand 1,4-bis(4-pyridyl)-benzene (dpb). The ligand dpypy can also act as a bidentate ligand rather than a tridentate building block as in **3**: thus, reaction of CuI with dpypy affords an additional product, **4**, that has been characterized as a one-dimensional chain constructed from trigonal planar Cu(I) centers bridged by terminally coordinated dpypy ligands. With the use of the ligand 5-(4-pyridyl)pyrimidine (pypm), an array of higher dimensionality has also been prepared: $[Cu_3I_3(pypm)]_\infty$ **5** represents the first example of a previously unknown type of copper iodide sheet with a 6^3 brick-wall type structure.[13]

Experimental Section

General. Ligands were prepared either by literature methods (dpt,[14] dpb[15]) or as described below using Suzuki coupling methodology. All other starting materials were purchased from Aldrich or Lancaster and used without further purification. ^{1}H NMR and elemental analysis measurements were performed at the University of Nottingham. Accurate mass spectrometry measurements were performed by electrospray techniques at the EPSRC National Mass Spectrometry Service Centre at Swansea University.

(4) (a) Li, D.; Wu, T.; Zhou, X. P.; Zhou, R.; Hitang, X. C. *Angew. Chem., Int. Ed.* **2005**, *44*, 4175. (b) Zhang, X. M.; Fang, R. Q.; Wu, H. S. *J. Am. Chem. Soc.* **2005**, *127*, 7670. (c) Long, D.-L.; Hill, R. J.; Blake, A. J.; Champness, N. R.; Hubberstey, P.; Proserpio, D. M.; Wilson, C.; Schröder, M. *Angew. Chem., Int. Ed.* **2004**, *43*, 1851. (d) Long, D.-L.; Blake, A. J.; Champness, N. R.; Wilson, C.; Schröder, M. *Angew. Chem., Int. Ed.* **2001**, *40*, 2444. (e) Long, D.-L.; Blake, A. J.; Champness, N. R.; Wilson, C.; Schröder, M. *Chem.—Eur. J.* **2002**, *8*, 2026.

(5) (a) Blake, A. J.; Brooks, N. R.; Champness, N. R.; Hanton, L. R.; Hubberstey, P.; Schröder, M. *Pure Appl. Chem.* **1998**, *70*, 2351. (b) Brooks, N. R.; Blake, A. J.; Champness, N. R.; Cooke, P. A.; Hubberstey, P.; Proserpio, D. M.; Wilson, C.; Schröder, M. *J. Chem. Soc., Dalton Trans.* **2001**, 456.

(6) (a) Hu, S.; Tong, M. L. *J. Chem. Soc., Dalton Trans*. **2005**, 1165. (b) Nather, C.; Wriedt, M.; Jess, I. *Inorg. Chem.* **2003**, *42*, 2391. (c) Nather, C.; Jess, I. *Inorg. Chem.* **2003**, *42*, 2968. (d) Pike, R. D.; Borne, B. D.; Maeyer, J. T.; Rheingold, A. L. *Inorg. Chem.* **2002**, *41*, 631. (e) Peng, R.; Wu, T.; Li, D. *CrystEngComm* [Online] **2005**, *7*, 595.

(7) (a) Blake, A. J.; Brooks, N. R.; Champness, N. R.; Crew, M.; Gregory, D. H.; Hubberstey, P.; Schröder, M.; Deveson, A.; Fenske, D.; Hanton, L. R. *Chem. Commun*. **2001**, 1432. (b) Blake, A. J.; Brooks, N. R.; Champness, N. R.; Cooke, P. A.; Crew, M.; Deveson, A. M.; Hanton, L. R.; Hubberstey, P.; Fenske, D.; Schöder, M. *Cryst. Eng*. **1999**, *2*, 181. (c) Blake, A. J.; Brooks, N. R.; Champness, N. R.; Cooke, P. A.; Deveson, A. M.; Fenske, D.; Hubberstey, P.; Li, W.-S.; Schröder, M. *J. Chem. Soc., Dalton Trans*. **1999**, 2103.

(8) (a) Barnett, S. A.; Blake, A. J.; Champness, N. R.; Wilson, C. *Chem. Commun*. **2002**, 1640. (b) Blake, A. J.; Champness, N. R.; Crew, M.; Hanton, L. R.; Parsons, S.; Schröder, M. *J. Chem. Soc., Dalton Trans.* **1998**, 1533. (c) Blake, A. J.; Brooks, N. R.; Champness, N. R.; Crew, M.; Hanton, L. R.; Hubberstey, P.; Parsons, S. M.; Schröder, M. *J. Chem Soc., Dalton Trans*. **1999**, 2813. (d) Barnett, S. A.; Blake, A. J.; Champness, N. R.; Wilson, C. *CrystEngComm* **2000**, *2*, 36.

(9) (a) Cariati, E.; Roberto, D.; Ugo, R.; Ford, P. C.; Galli, S.; Sironi, A. *Inorg. Chem*. **2005**, *44*, 4077. (b) Vitale, M.; Ford, P. C. *Coord. Chem. Rev.* **2001**, *219*, 3.

(10) (a) Amoore, J. J. M.; Hanton, L. R.; Spicer, M. D. *J. Chem. Soc., Dalton Trans*. **2003**, 1056. (b) Caradoc-Davies, P. L.; Gregory, D. H.; Hanton, L. R.; Turnbull, J. M. *J. Chem. Soc., Dalton Trans.* **2002**, 1574. (c) Yaghi, O. M.; Li, G. *Angew. Chem., Int. Ed. Engl*. **1995**, *34*, 207. (d) Hu, S.; Chen, J.-C.; Tong, M.-L.; Wang, B.; Yan, Y.-X.; Batten, S. R. *Angew. Chem., Int. Ed.* **2005**, *44*, 5471.

(11) (a) Caradoc-Davies, P. L.; Hanton, L. R.; Hodgkiss, J. M.; Spicer, M. D. *J. Chem. Soc., Dalton Trans.* **2002**, 1581. (b) Kuhn, N.; Fawzi, R.; Grathwohl, M.; Kotowski, H.; Steimann, M. *Z. Anorg. Allg. Chem.* **1998**, *624*, 1937. (c) Su, C.-Y.; Kang, B.-S.; Sun, J. *Chem. Lett.* **1997**, 821. (d) Dai, J.; Munakata, M.; Wu, L.-P.; Kuroda-Sowa, T.; Suenaga, Y. *Inorg. Chim. Acta* **1997**, *258*, 65. (e) Graham, A. J.; Healy, P. C.; Kildea, J. D.; White, A. H. *Aust. J. Chem*. **1989**, *42*, 177. (f) Healy, P. C.; Kildea, J. D.; White, A. H. *J. Chem. Soc., Dalton Trans*. **1988**, 1637. (g) Rath, N. P.; Holt, E. M.; Tanimura, K. *J. Chem. Soc., Dalton Trans*. **1986**, 2303. (h) Healy, P. C.; Pakawatchai, C.; Raston, C. L.; Skelton, B. W.; White, A. H. *J. Chem. Soc., Dalton Trans.* **1983**, 1905. (i) Churchill, M. R.; DeBoer, B. G.; Donovan, D. J. *Inorg. Chem*. **1975**, *14*, 617. (j) Li, G.; Shi, Z.; Liu, X.; Dai, Z.; Feng, S. *Inorg. Chem.* **2004**, *43*, 6884.

(12) (a) Barnett, S. A.; Blake, A. J.; Champness, N. R.; Nicolson, J. E. B.; Wilson, C. *J. Chem. Soc., Dalton Trans.* **2001**, 567. (b) Sasa, M.; Tanaka, K.; Bu, X.-H.; Shiro, M.; Shionoya, M. *J. Am. Chem. Soc.* **2001**, *123*, 10750. (c) In this article, the term angular ligand is used to describe a bridging ligand in which the donor atoms are disposed at a defined angle with respect to each other (see ref 11).

(13) For an excellent introduction to network structures and topology we would encourage readers to study the following. *Molecule-Based Materials: The Structural Network Approach;* Öhrström, L., Larsson, K. Eds.; Elsevier: Amsterdam, 2005.

(14) Fischer, H.; Summers, L. A. *Tetrahedron* **1976**, *32*, 615.

(15) Biradha, K.; Fujita, M. *J. Chem. Soc., Dalton Trans.* **2000**, 3805.

An alternative but similar preparation route for the ligand dpypy is available in the literature.[16]

5-(4-Pyridyl)pyrimidine (pypm). 4-(4,4,5,5-Tetramethyl-1,3,2-dioxaborolan-2-yl)-pyridine[17] (2.05 g, 10 mmol), 5-bromopyrimidine (1.6 g, 10 mmol), cesium carbonate (5 g, 15 mmol), and tetrakis(triphenylphosphine)palladium(0) (0.115 g, 0.1 mmol) were added to 100 cm^3 of deoxygenated DMF in a 250 cm^3 three-necked, round-bottom flask equipped with a condenser and containing a nitrogen atmosphere. The solution was protected from light with aluminum foil and heated in an oil bath at 95 °C for 8 days. DMF was then removed by evaporation, and the product was separated by column chromatography on silica gel 60 using water as the eluent (white powder, yield 1.30 g, 83%). Found (calcd for $C_{18}H_{16}N_6O$ {pypm·0.5H_2O}) (%): C, 65.39 (65.06); H, 4.44 (4.82); N, 24.15 (25.30). ^{1}H NMR ($CDCl_3$, δ in ppm): 9.33 (s, 1 H), 9.03 (s, 2 H), 8.80 (dd, 2 H, $J_1 = 2.8$ Hz, $J_2 = 1.7$ Hz), 7.54 (dd, 2 H, $J_1 = 2.8$ Hz, $J_2 = 1.6$ Hz). ^{13}C NMR ($CDCl_3$, δ in ppm): 158.8, 155.0, 150.6, 141.9, 131.6, 121.4. IR (KBr) (cm^{-1}): 3039 (w), 1704 (w), 1603 (m), 1568 (m), 1416 (m), 1327 (w), 1293 (w), 1221 (w), 1128 (w), 1059 (w), 993 (w), 923 (w), 819 (m), 780 (w), 724 (m), 631 (w), 586 (m). Accurate mass spectrometry (AMS) $[M + H]^+$, found (calcd): 158.0715 (158.0713).

3,5-Bis(4-pyridyl)-pyridine (dpypy). 4-(4,4,5,5-Tetramethyl-1,3,2-dioxaborolan-2-yl)-pyridine[17] (2.05 g, 10 mmol), 3,5-dibromopyridine (1.18 g, 5 mmol), cesium carbonate (5 g, 15 mmol), and tetrakis(triphenylphosphine)palladium(0) (0.115 g, 0.1 mmol) were added in 100 cm^3 of deoxygenized toluene/ethanol (95/5) in a 250 cm^3 three-necked, round-bottom flask equipped with a condenser and containing a nitrogen atmosphere. The solution was protected from light with aluminum foil and heated at 95 °C for 8 days using an oil bath. The solvent was then evaporated, and the product was separated by column chromatography on silica gel 60 using acetone as the eluent (white powder, yield 0.63 g, 54%). Found (calcd for $C_{22}H_{19}N_3$ {dpypy·C_6H_5Me}) (%): C, 82.49 (81.23); H, 5.17 (5.85); N, 12.33 (12.92). Repeated attempts to obtain satisfactory elemental analysis for samples of dpypy were unsuccessful because of varying degrees of solvation by a variety of solvent species. ^{1}H NMR ($CDCl_3$, δ in ppm): 8.98 (d, 2 H, $J =$ 2.2 Hz), 8.79 (dd, 4 H), 8.15 (t, 1 H, $J = 2.2$ Hz), 7.60 (dd, 4 H, $J_1 = 2.8$ Hz, $J_2 = 1.7$ Hz). ^{13}C NMR ($CDCl_3$, δ in ppm): 151.7, 148.4, 144.7, 134.3, 132.8, 121.7. IR (KBr) (cm^{-1}): 3028 (w), 1603 (m, 1551 (w), 1402 (m), 1322 (w), 1222 (w), 1026 (w), 992 (w), 917 (w), 815 (s), 715 (m), 627 (w), 543 (m). AMS $[M + H]^+$, found (calcd): 234.1026 (234.1026).

[(CuI)(dpt)·MeCN]$_\infty$ (1). A solution of dpt (93 mg, 0.40 mmol) in CH_2Cl_2 (3 cm^3) was added to a cooled solution of CuI (76 mg, 0.40 mmol) dissolved in hot MeCN (20 cm^3). The reddish-brown precipitate that formed immediately was collected by filtration and dried in vacuo. Yield 89%. Found (calcd for $C_{13}H_9CuIN_5$ [(CuI)(dpt)]) (%): C, 37.39 (36.68); H, 2.07 (2.14); N, 16.33 (16.46). IR (KBr) (cm^{-1}): 2966 (w), 2955 (w), 2848 (w), 1655 (w), 1637 (w), 1567 (m), 1528 (s), 1508 (m), 1417 (s), 1385 (m), 1317 (w), 1300 (w), 1261 (w), 1055 (w), 798 (m), 671 (w), 650 (w), 419 (m). Crystals suitable for single-crystal X-ray diffraction were prepared by the slow diffusion of a solution of CuI in MeCN into a solution of dpt in CH_2Cl_2.

[CuI(dpb)]$_\infty$ (2). Compound **2** was prepared by the slow diffusion of solutions of dpb (5 mg, 0.01 mmol) and CuI (15 mg, 0.01 mmol) in MeCN (2 cm^3). Each solution was placed in a vial (volume of 2 cm^3) which was in turn placed in a larger vial (volume of 10 cm^3) which was carefully filled with MeCN to avoid rapid mixing of the two reagent solutions. Orange crystals of **3** grew in the ligand-rich region of the layering experiment, and yellow crystals grew in the metal-rich region. A pure phase of **2** could also be prepared by precipitation from rapidly mixed solutions of dpb and CuI (1:1 stoichiometry) in MeCN. Yield 27%. Found (calcd for $C_{16}H_{12}CuIN_2$ [(CuI)(dpb)]) (%): C, 45.40 (45.45); H, 2.63 (2.84); N, 6.38 (6.63). IR (KBr) (cm^{-1}): 3073 (w), 1592 (m), 1549 (m), 1481 (m), 1420 (m), 1404 (m), 1230 (m), 1042 (w), 991 (w), 797 (s), 704 (m), 586 (m), 461 (w).

Table 1. Selected Bond Lengths (Å) and Angles (deg) for [(CuI)(dpt)]$_\infty$ (**1**) and [CuI(dpb)]$_\infty$ (**2**)[a]

1		**2**	
Cu1−N1	2.037(3)	Cu1−I1	2.6094(4)
Cu1−N16^{i}	2.050(3)	Cu1−N1	2.074(2)
Cu1−I1	2.6236(7)		
Cu1−I2	2.7266(8)		
Cu2−N21	2.033(4)		
Cu2−N36^{i}	2.037(4)		
Cu2−I2	2.6382(8)		
Cu2−I1	2.6956(8)		
N1−Cu1−N16^{i}	121.36(14)	N1−Cu1−N1^{i}	101.20(14)
N1−Cu1−I1	109.78(10)	N1−Cu1−I1^{ii}	109.61(7)
N16^{i}−Cu1−I1	109.70(10)	N1−Cu1−I1	114.15(7)
N1−Cu1−I2	105.24(9)	N1^{i}−Cu1−I1	109.61(7)
N16^{i}−Cu1−I2	105.33(10)	I1−Cu1−I1^{ii}	108.17(2)
I1−Cu1−I2	103.82(2)		
N21−Cu2−N36^{i}	120.29(15)		
N21−Cu2−I2	109.09(10)		
N36^{i}−Cu2−I2	108.72(10)		
N21−Cu2−I1	105.33(10)		
N36^{i}−Cu2−I1	107.95(10)		
I2−Cu2−I1	104.28(2)		

[a] Symmetry transformations used to generate equivalent atoms. **1**: (i) x, $y + 1$, $z - 1$. **2**: (i) $-x + {}^1/_2$, $-y - {}^1/_2$, z; (ii) x, $y - 1$, z.

[CuI(dpypy)]$_\infty$ (3, **4)**. The dpypy (5 mg, 0.01 mmol) and CuI (15 mg, 0.01 mmol) were dissolved in DMF (2 cm^3) and stirred for 5 min. The solution was then placed in a steel autoclave which was heated at 150 °C for 5 days. After the autoclave was cooled, the sample was retrieved as orange columnar crystals in 95% yield. Attempts to obtain CHN elemental analysis were unsuccessful because of the mixture of phases obtained (see Results and Discussion).

{**Cu_3I_3(pypm)**}$_\infty$ **(5)**. CuI (30 mg) and 5-(4-pyridyl)-pyrimidine (30 mg) were added to a water/acetonitrile solution (50/50, 5 cm^3) and stirred for 5 min. The solution was then placed in a steel autoclave and heated at 120 °C for 5 days. Orange crystalline needles formed at the bottom of the vial: these were extracted from the solution and stored in *n*-hexane. Found (calcd for $C_9H_7Cu_3I_3N_3$ {Cu_3I_3(5-pypm)}$_\infty$]) (%): C, 15.38 (14.83); H, 0.78 (0.96); N, 5.86 (5.77). IR (KBr) (cm^{-1}): 1608 (m), 1574 (m), 1413 (m), 1403 (s), 1351 (w), 1322 (w), 1174 (w), 1068 (w), 1009 (w), 916 (w), 824 (s), 801 (w), 669 (w), 651 (w), 585 (w), 564 (m).

X-ray Crystallographic Studies. Single crystal X-ray data collections were performed on a Bruker SMART1000 (**1**), on a Bruker SMART APEX CCD area detector diffractometer for **2**−**5**, and on a Bruker-Nonius kappaCCD area detector diffractometer for pypm·H_2O. Structures were solved by direct methods using SHELXS97,[18] and full-matrix least squares refinement employed

(16) Kubota, Y.; Biradha, K.; Fujita, M.; Sakamoto, S.; Yamaguchi, K. *Bull. Chem. Soc. Jpn.* **2002**, *75*, 559.
(17) Coudret, C. *Synth. Commun.* **1996**, *26*, 3543.
(18) Sheldrick, G. M. *SHELXS97*; University of Göttingen: Göttingen, Germany, 1997.

Table 2. Selected Bond Lengths (Å) and Angles (deg) for $[(CuI)_3(dpypy)_2]_\infty$ (**3**), $[CuI(dpypy)]_\infty$ (**4**), and $\{Cu_3I_3(5\text{-pypm})\}_\infty$ (**5**)[a]

3

Cu1−I1	2.650(2)	N11^{i}−Cu1−N8	115.3(7)	N7^{ii}−Cu5−N9	121.5(6)
Cu1−I2	2.632(3)	N11^{i}−Cu1−I2	105.1(4)	N7^{ii}−Cu5−I5	110.5(4)
Cu1−N8	2.043(15)	N8−Cu1−I2	109.5(5)	N9−Cu5−I5	110.5(4)
Cu1−N11^{i}	2.029(14)	N11^{i}−Cu1−I1	104.6(4)	N7^{ii}−Cu5−I6	106.7(4)
Cu2−I1	2.683(2)	N8−Cu1−I1	110.1(4)	N9−Cu5−I6	106.7(4)
Cu2−I2	2.680(2)	I2−Cu1−I1	112.14(9)	I5−Cu5−I6	98.15(8)
Cu2−N2	2.050(14)	N2−Cu2−N5	125.6(6)	N12−Cu6−N10^{ii}	122.1(6)
Cu2−N5	2.063(14)	N2−Cu2−I2	104.3(4)	N12−Cu6−I5	110.7(5)
Cu3−I3	2.638(3)	N5−Cu2−I2	106.2(4)	N10^{ii}−Cu6−I5	110.2(4)
Cu3−I4	2.638(3)	N2−Cu2−I1	104.9(4)	N12−Cu6−I6	106.3(4)
Cu3−N4^{ii}	2.038(15)	N5−Cu2−I1	105.7(4)	N10^{ii}−Cu6−I6	105.9(4)
Cu3−N6	2.045(14)	I2−Cu2−I1	109.64(9)	I5−Cu6−I6	98.76(8)
Cu4−I3	2.737(3)	N4^{ii}−Cu3−N6	122.5(6)		
Cu4−I4	2.653(3)	N4^{ii}−Cu3−I3	108.0(4)		
Cu4−N1^{iii}	2.055(14)	N6−Cu3−I3	106.8(4)		
Cu4−N3^{iv}	2.021(14)	N4^{ii}−Cu3−I4	103.3(4)		
Cu5−I5	2.678(3)	N6−Cu3−I4	102.5(4)		
Cu5−I6	2.710(3)	I3−Cu3−I4	113.88(9)		
Cu5−N7^{ii}	2.018(15)	N3^{iv}−Cu4−N1^{iii}	122.6(6)		
Cu5−N9	2.028(15)	N3^{iv}−Cu4−I4	105.9(4)		
Cu6−I5	2.672(3)	N1^{iii}−Cu4−I4	105.5(4)		
Cu6−I6	2.692(3)	N3^{iv}−Cu4−I3	105.7(4)		
Cu6−N12	1.999(15)	N1^{iii}−Cu4−I3	106.6(4)		
Cu6−N10^{ii}	2.025(14)	I4−Cu4−I3	110.24(9)		

4

Cu−N1	1.979(3)	N1−Cu−N1^{i}	127.83(16)
Cu−I	2.5415(8)	N1−Cu−I	116.09(8)

5

Cu1−N11	2.076(3)	N11−Cu1−I1^{i}	121.40(9)	N1^{iii}−Cu3−I2	109.55(10)
Cu1−I1^{i}	2.5964(7)	N11−Cu1−I2^{i}	107.03(9)	N1^{iii}−Cu3−I3	110.87(10)
Cu1−I2^{i}	2.6491(7)	I1^{i}−Cu1−I2^{i}	108.91(3)	I2−Cu3−I3	119.88(2)
Cu1−I1	2.7345(9)	N11−Cu1−I1	100.67(10)	N1^{iii}−Cu3−I3^{iv}	101.20(10)
Cu2−N9^{ii}	2.057(3)	I1−Cu1−I1^{i}	107.06(2)	I2−Cu3−I3^{iv}	110.88(2)
Cu2−I3	2.5823(8)	I2−Cu1−I1^{i}	111.47(2)	I3−Cu3−I3^{iv}	102.67(3)
Cu2−I1	2.6630(7)	N9^{ii}−Cu2−I3	116.05(10)		
Cu2−I2	2.8046(8)	N9^{ii}−Cu2−I1	114.43(9)		
Cu3−N1^{iii}	2.035(3)	I3−Cu2−I1	108.37(2)		
Cu3−I2	2.6186(8)	N9^{ii}−Cu2−I2	98.86(9)		
Cu3−I3	2.6517(7)	I3−Cu2−I2	115.67(2)		
Cu3−I3^{iv}	2.7167(8)	I1−Cu2−I2	102.60(3)		

[a] Symmetry transformations used to generate equivalent atoms. **3**: (i) $x, y+1, z$; (ii) $x+1, y, z$; (iii) $x+1, y-1, z$; (iv) $x, y-1, z$. **4**: (i) $1-x, y, -z+{}^3/_2$. **5**: (i) $-x, 1-y, -z$; (ii) $-x, 1-y, -1-z$; (iii) $-1-x, {}^3/_2-y, {}^1/_2-z$; (iv) $x, {}^3/_2-y, {}^1/_2-z$.

Table 3. Crystallographic Data Summary for Complexes **1**−**5** and pypm·H_2O

	1	**2**	**3**	**4**	**5**	pypm·H_2O
formula	$C_{28}H_{21}Cu_2I_2N_{11}$	$C_{16}H_{12}CuIN_2$	$C_{60}H_{44}Cu_6I_6N_{12}$	$C_{15}H_{11}CuIN_3$	$C_9H_7Cu_3I_3N_3$	$C_{18}H_{18}N_6O_2$
mol wt	892.44	422.72	2075.71	423.71	728.50	349.38
cryst syst	triclinic	orthorhombic	monoclinic	orthorhombic	monoclinic	monoclinic
space group	$P\bar{1}$	*Pccn*	*P2/c*	*Pbcn*	$P2_1/c$	*C2/c*
a (Å)	10.988(2)	21.618(3)	13.624(2)	9.040(2)	8.643(2)	38.565(8)
b (Å)	12.236(3)	4.2267(7)	16.235(3)	14.870(3)	20.034(5)	3.7140(7)
c (Å)	12.292(3)	15.212(2)	30.292(5)	10.270(2)	8.384(2)	29.750(6)
α (deg)	65.459(3)					
β (deg)	77.598(4)		100.617(2)		99.846(4)	126.78(3)
γ (deg)	85.232(4)					
U (Å^3)	1468.2(6)	1389.9(4)	6585.7(18)	1380.5(5)	1430.3(6)	3413.1(12)
Z	2	4	4	4	4	8
T (K)	150(2)	150(2)	150(2)	150(2)	150(2)	120(2)
μ (mm^{-1})	3.592	3.782	4.763	3.810	10.878	0.094
reflns collected	6739	8516	14334	7603	12256	23844
unique reflns (R_{int})	4478 (0.061)	1614 (0.034)	6713 (0.071)	1101 (0.0511)	3222 (0.087)	3929 (0.105)
final R_1 [$F > 4\sigma(F)$]	0.0359	0.0252	0.0858	0.0295	0.0229	0.0786
wR2 (all data)	0.0755	0.0571	0.264	0.0603	0.0496	0.133

SHELXL97.[19] All hydrogen atoms were placed in geometrically calculated positions and thereafter refined using a riding model with $U_{iso}(H) = 1.2U_{eq}(C)$. All non-hydrogen atoms were refined with anisotropic displacement parameters. Other details of crystal data and structure determination are given in Table 3. Powder X-ray diffraction patterns were collected using a Philips X'pert $\theta-2\theta$ diffractometer with Cu Kα radiation from samples mounted on flat glass plate sample holders. Scans of approximately 50 min were

(19) Sheldrick, G. M. *SHELXL97*; University of Göttingen: Göttingen, Germany, 1997.

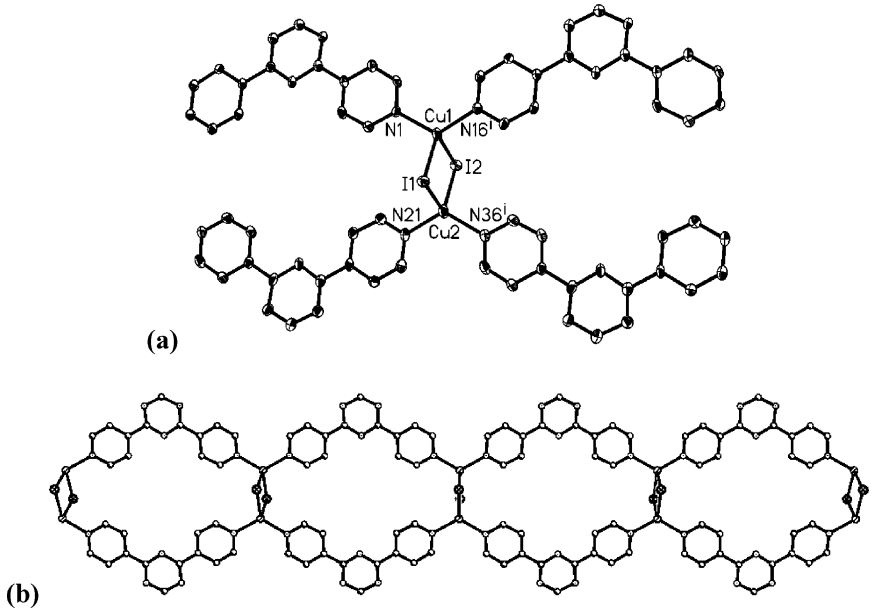

Figure 1. (a) View of the Cu(I) coordination environment found in $[CuI(dpt)\cdot MeCN]_\infty$, **1**, showing the numbering scheme used. The displacement ellipsoids are drawn at the 50% probability level. (b) View of the ribbon structure found for $[CuI(dpt)]_\infty$. Hydrogen atoms and MeCN solvent molecules are omitted for clarity. The symmetry code (i) correspnds to $x, y + 1, z - 1$.

run for each sample to assess phase purity and were run over the range $5° \leq 2\theta \leq 80°$ with a step size of 0.02° in 2θ and a step time of 0.65 s. Simulated powder patterns were generated using either APD (part of the Philips software package) or POWDER-CELL,[20] taking the final model from single-crystal structure refinement as input.

Results and Discussion

The ligands illustrated in Chart 1 were reacted with CuI under a range of conditions to afford CuI−ligand coordination polymers with a variety of structures and $(CuI)_\infty$ motifs.

$[CuI(dpt)\cdot MeCN]_\infty$ (1). Slow diffusion of a solution of the angular ligand dpt dissolved in CH_2Cl_2 into a solution of CuI in MeCN in the L/M ratios of 1:1 and 1:2 gave dark red crystals of the coordination polymer $[CuI(dpt)\cdot MeCN]_\infty$, **1**. A single-crystal structure determination of **1** reveals that each approximately tetrahedral Cu(I) center is bound by two iodide anions and two dpt ligands (Figure 1a; see Table 1 for selected bond lengths and angles) which results in a planar ribbon-type structure with dpt acting as a bidentate ligand connected via $[Cu_2I_2]$ rhomboid dimer cores. These metal−iodide cores act as planar, four-connected junctions that are joined to each other via two dpt ligands (Figure 1b). The ribbon structure in **1** is very similar to that observed in $[CuI(bis(4\text{-pyridyl})disulfide)]_\infty$.[7a] The choice of the angular ligand dpt incorporating a relative disposition of a 120° angle between the pyridyl N-donors results in the formation of cavities in **1** which are bordered by the organic ligands and $[Cu_2I_2]$ units. The distance between the centroids of the $[Cu_2I_2]$ cores is 13.26 Å, and the N···N distance between the nitrogens of the triazine rings across a cavity is 7.94 Å. Although this means the cavities are large enough to accommodate guest molecules, the packing arrangement of the ribbons precludes the possibility of inclusion because of dpt ligands from adjacent ribbons sitting above and below the cavity within a given ribbon. However, MeCN solvent molecules do occupy the residual space between the layers of ribbons. It is particularly notable in the context of this paper, and in particular for compounds **3** and **4**, that the triazine N-donors of the dpt ligand are not coordinated to any Cu(I) centers in **1**. This concurs with previously observed complexes of the ligand dpt[8a,12] and with the relatively hindered nature and poor donor ability of its triazine N-donors.

Attempts to obtain bulk samples of **1** by rapid precipitation revealed that only a reaction with a dpt and CuI in a 1:1 ratio yielded the red complex **1** (Figure 2). A reaction using a 1:2 dpt/CuI ratio gave a brown powder which was shown by powder X-ray diffraction (Figure 2) to be a mixture of **1** and another product. Elemental analysis indicated that the latter was most likely to be a complex with formula $[(CuI)_2(dpt)]_\infty$, but unfortunately, attempts to grow single crystals have been unsuccessful thus far.

$[CuI(dpb)]_\infty$ (2). Compound **2** can be prepared either via rapid precipitation by mixing solutions of CuI and dpb in a 1:1 stoichiometric ratio or by layering MeCN solutions of the ligand and metal salt. Whereas the rapid precipitation method affords a pure phase of **2**, as shown by powder X-ray diffraction, layering methods give two distinct forms. Orange crystals of **2** are grown in the ligand-rich region of the layering experiment, while yellow crystals appear in the metal-rich region. Unfortunately, the yellow crystals were not of sufficient quality or quantity to allow structural determination of this other product. However, the observation of the yellow phase is entirely consistent with previous observations with other linear dipyridyl ligands where both orange and yellow forms are commonly observed.[7b] In other instances, the yellow form has been found to have a stoichiometry of $[(CuI)_2L)]_\infty$ and a structure based on CuI

(20) Nolze, G.; Kraus, W. *Powder Diffr.* **1998**, *13*, 256.

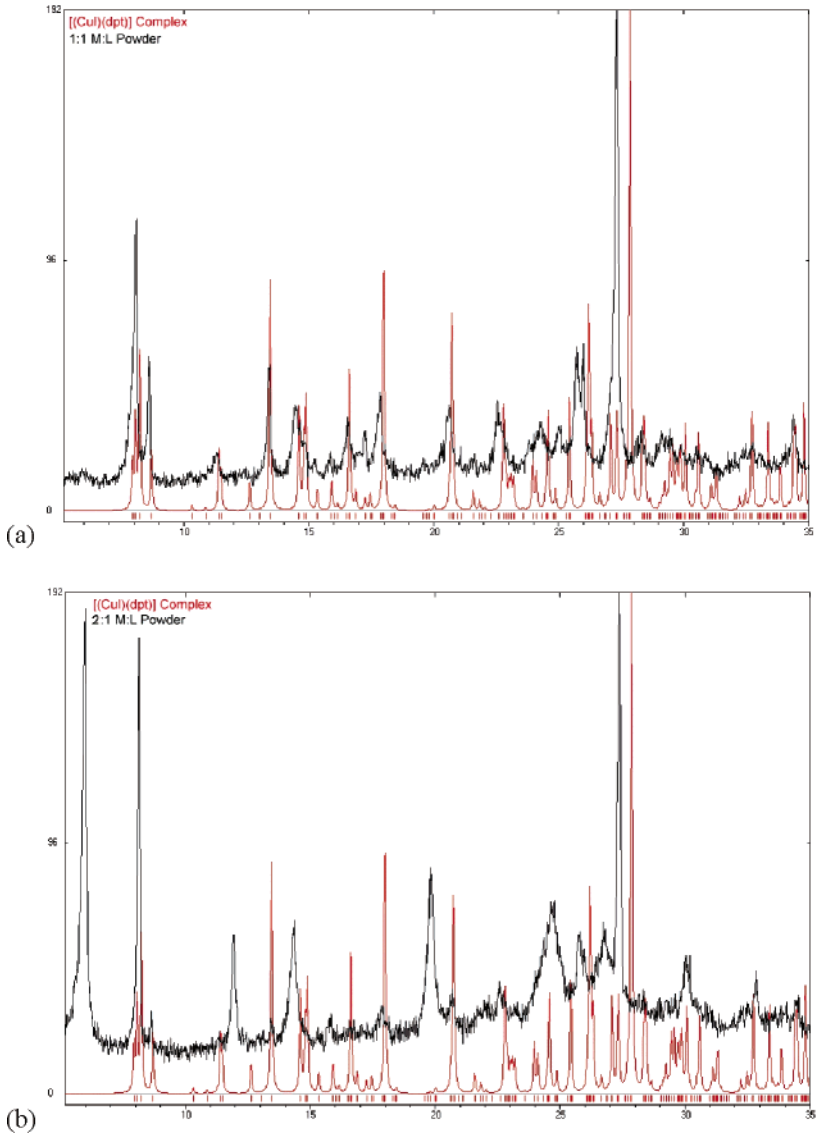

Figure 2. (a) The powder X-ray diffraction pattern observed from the 1:1 CuI/dpt reaction showing the observed data (black line) and the calculated pattern from the single-crystal X-ray data for $[(CuI)(dpt)\cdot MeCN]_\infty$, **1** (red line). (b) The powder pattern observed from the 1:2 dpt/CuI reaction showing the observed data (black line) and the calculated pattern from the single-crystal X-ray data for $[(CuI)(dpt)\cdot MeCN]_\infty$, **1** (red line), see text.

ladders linked by dipyridyl ligands to afford a two-dimensional sheet structure.[7b]

The importance of the angular nature of dpt is clearly shown by the structure of **2** formed by the linear ligand dpb. Dpb consists of three aromatic units, but in this case the central unit is substituted in its para positions, and so the ligand acts as a simple linear connector. As has been observed previously, one-dimensional $(CuI)_\infty$ chains or ladders are typically observed with linear ligands of this type.[7b] This trend is followed by **2** in which undulating two-dimensional sheets are observed with dpb ligands linking $(CuI)_\infty$ chains (Figure 3a) and each Cu(I) center being coordinated by two iodides and two pyridyl donors (Figure 3b; see Table 1 for selected bond lengths and angles). Previous observations have indicated that $(CuI)_\infty$ chains are favored by bipyridyl ligands containing multiple aromatic rings.[7b] However, despite the observation of $(CuI)_\infty$ chains in **2**, no $\pi-\pi$ stacking interactions are observed between adjacent dpb ligands, with a minimum centroid−centroid distance of 4.23 Å seen between phenylene or pyridyl rings of adjacent ligands.

$[(CuI)_3(dpypy)_2]_\infty$ (3) and $[CuI(dpypy)]_\infty$ (4). Compounds **3** and **4** were prepared by solvothermal methods using either DMF or a 1:1 DMF/H_2O mixture as solvent. Using this approach, dpypy reacts with CuI to afford three distinct crystalline products, including **3** and **4**, all orange in color and with no distinct morphological differences. A third phase was isolated as a single crystal, but although a monoclinic unit cell [a = 18.544(3) Å, b = 17.308(3) Å, and c = 14.583(2) Å, β = 113.54(3)°] could be determined, no chemically sensible structure solution could be obtained from the diffraction data collected. Powder X-ray diffraction measurements were performed upon bulk materials isolated from the reaction between dpypy and CuI. The diffractogram showed that the powder obtained is mostly amorphous and that although some peaks can be identified as being due to **3** or **4**, other peaks indicate the presence of other phases that have not been isolated as single crystals.

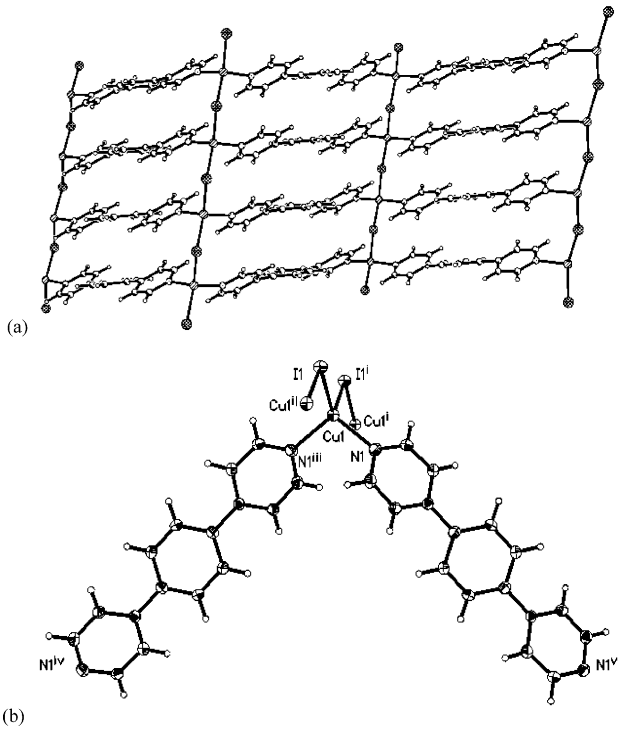

Figure 3. (a) View of the two-dimensional sheet observed in **2** illustrating the bridging of $(CuI)_\infty$ chains by the linear dpb ligands. (b) View of the Cu(I) coordination environment found in **2**, showing the numbering scheme used. Displacement ellipsoids are drawn at the 50% probability level. The symmetry codes are as follows: (i) $x, y - 1, z$; (ii) $x, y + 1, z$; (iii) $-x, y - {}^1/_2, -z + {}^1/_2$; (iv) $x + {}^1/_2, 1 - y, -z + {}^5/_2$; (v) $-x + {}^3/_2, -y - {}^1/_2, z + 2$.

Compound **3** adopts an unusual two-dimensional bilayer sheet that uses all three ligand N-donors of dypy (Figure 4a; see Table 1 for selected bond lengths and angles). In each case a $(CuI)_2$ rhomboid dimer is formed, and ribbon structures similar to those observed in **1** are generated. These ribbons are then linked via $(CuI)_2$ coordination at the central pyridyl donor unit to afford a two-dimensional structure of linked ribbons (Figure 4b). The ligand acceptor sites of this $(CuI)_2$ dimeric unit are oriented such that the formation of a bilayer structure is favored (Figure 4b). These bilayers are then interpenetrated by an adjacent layer such that bilayers of bilayers are formed (Figure 4c). Such interpenetrated two-dimensional structures have been observed previously,[21] but the interpenetration of bilayer structures is significantly less common.[22] Interpenetrating layers interact via $\pi-\pi$ stacking interactions between pyridyl groups of dpypy ligands on separate $[CuI(dpypy)]_\infty$ bilayers (centroid−centroid separation 3.82 Å, offset 1.72 Å).

Compound **4**, $[CuI(dpypy)]_\infty$, also prepared from CuI and dpypy under solvothermal conditions, shows an entirely different structure to that observed in **3**. In **4** each Cu(I) center adopts a trigonal planar geometry, coordinated by two pyridyl donors from two spatially distinct dpypy ligands and from a nonbridging iodide ligand (see Table 2 for selected bond lengths and angles, Figure 5). The dpypy ligands bridge Cu-

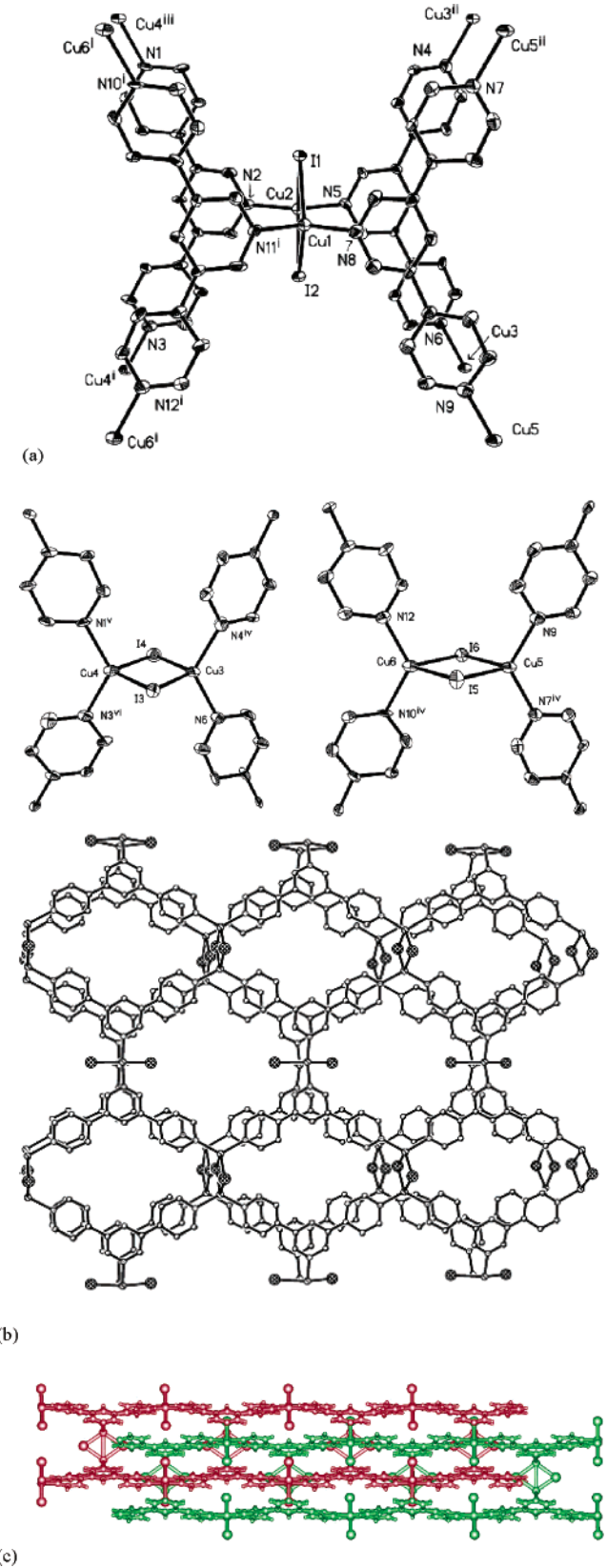

Figure 4. (a) View of the Cu(I) coordination environments found in **3**, showing the numbering schemes used. Displacement ellipsoids are drawn at the 50% probability level. The symmetry codes are as follows: (i) $x, 1 + y, z$; (ii) $x - 1, y, z$; (iii) $x - 1, y + 1, z$; (iv) $x + 1, y, z$; (v) $x + 1, y - 1, z$; (vi) $x, y - 1, z$. (b) View of the bilayer structure observed in **3**: note the orientations of $(CuI)_2$ rhomboid dimers (Cu, right hatch; N, dotted; I, black, filled circles). (c) View of the interpenetrated bilayers observed in **3**.

(21) Batten, S. R. *CrystEngComm* **2001**, *3*, 67.
(22) Sun, D. F.; Bi, W. H.; Li, X.; Cao, R. *Inorg. Chem. Commun.* **2004**, *7*, 683.

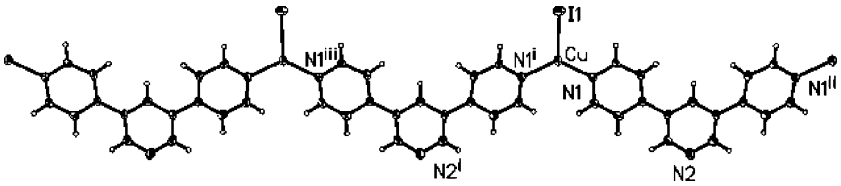

Figure 5. A view of **4** showing the Cu(I) coordination environment, the one-dimensional chain structure, and the atom numbering scheme. Displacement ellipsoids are drawn at the 50% probability level. The symmetry codes are as follows: (i) $1 - x, y, -z + {}^3/_2$; (ii) $-x, -y, 2 - z$; (iii) $1 + x, y, z - 1$.

(I) centers as a bidentate donor to generate a one-dimensional chain structure with the central pyridyl donor of the dpypy ligands remaining uncoordinated. Although chains are arranged in a parallel fashion in the *ac* plane, adjacent sheets of parallel chains are organized such that chains in neighboring sheets are orthogonal to one another. Adjacent chains interact via two different, but long, $\pi-\pi$ interactions: the first between two coordinated pyridyl rings (centroid−plane distance = 3.452 Å; centroid−centroid distance = 4.069 Å), the second between a coordinated pyridyl ring and an uncoordinated central dpypy ring (centroid−plane distance = 3.494 Å; centroid−centroid distance = 4.154 Å). Although nonbridging iodides with a trigonal planar geometry[23] are unusual for copper iodide species, this geometrical arrangement is relatively common for Cu(I) complexes.

$[Cu_3I_3(pypm)]_\infty$ (5). Single crystals of compound **5** were prepared using solvothermal synthetic methods by reacting copper(I) iodide with pypm at 120 °C for 5 days in a water/acetonitrile (1:1) solution. Attempts to prepare samples of **5** by precipitation from rapidly mixed solutions of CuI and pypm in MeCN gave only amorphous material as evidenced by powder X-ray diffraction.

A single-crystal structural determination of **5** reveals a three-dimensional structure in which highly unusual $(CuI)_\infty$ sheets are pillared by pypm ligands (Figure 6a). Each N-donor of the pypm ligand is coordinated to a Cu(I) cation which forms part of the extended $(CuI)_\infty$ sheet structure (Figure 6b; see Table 2 for selected bond lengths and angles). The $(CuI)_\infty$ sheet (Figure 6c) comprises $(CuI)_\infty$ chains (green, Figure 6c) that are cross-linked by $(CuI)_4$ stepped cubane tetramers (red in Figure 6c)[10] to give an overall 6^3 net. Although a range of $(CuI)_\infty$ structures have been reported ranging from zero- to three-dimensional structures (see Introduction), this type of $(CuI)_\infty$ sheet structure is highly unusual and, to our knowledge, unprecedented. The pypm ligands bridge adjacent $(CuI)_\infty$ sheets such that for a given pypm ligand the pyrimidine group sits within a pore of one sheet and acts as a bridge across the pore to another sheet (Figure 7). The pyridine donor of the ligand binds to copper centers within $(CuI)_\infty$ chains (highlighted in green in Figure 6c) on an adjacent sheet.

The single crystal structure of the monohydrated form of the free ligand (pypm·H_2O) was also collected to serve as a comparison with the structure of **5**. In the structure of pypm·H_2O each pypm molecule participates in N···H−O hydrogen bonding with a water molecule [H···N = 2.04(5) Å; O···N = 2.813(6) Å; O−H···N = 151(6)°] through the pyridine N-atom while the pyrimidine N-donors form C−H···N intermolecular interactions with adjacent pyrimidine groups [H···N = 2.590 Å; C···N = 3.517(4) Å; C−H···N = 163°]. Interestingly, the average dihedral angle between the pyrimidine ring and the pyridyl ring of the pypm molecules in

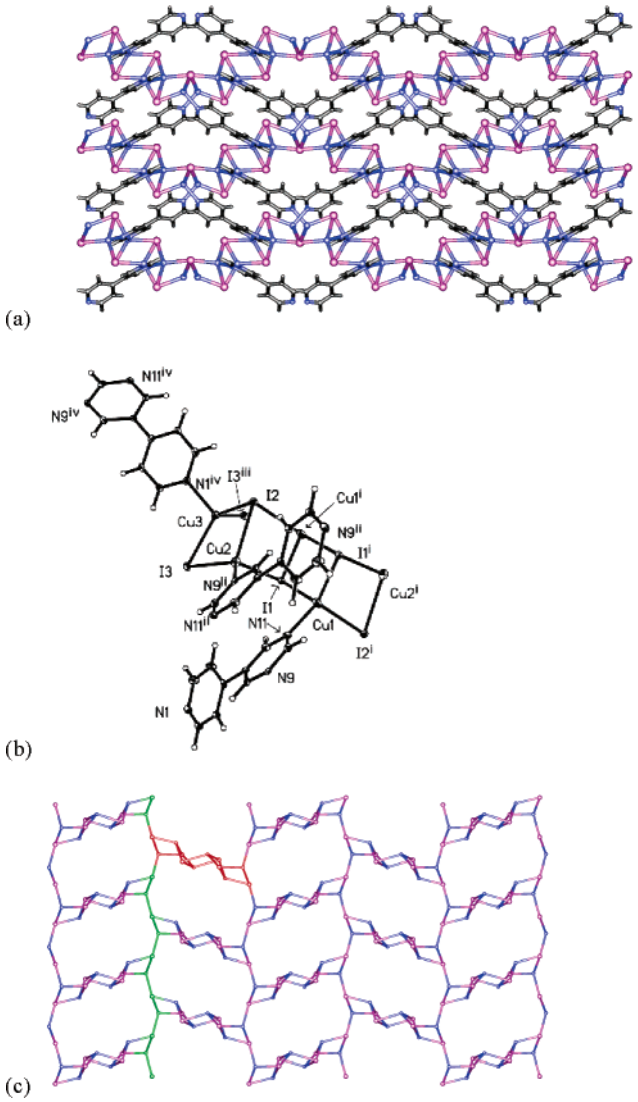

Figure 6. (a) View of the three-dimensional structure of **5** in which $(CuI)_\infty$ sheets are pillared by pypm ligands (Cu, blue; I, purple; N, blue; C, gray). (b) View of the Cu(I) coordination environment found in **5**, showing the numbering scheme used. Displacement ellipsoids are drawn at the 50% probability level. The symmetry codes are as follows: (i) $-x, y + {}^3/_2, -z + {}^1/_2$; (ii) $-x, y + {}^3/_2, -z - {}^1/_2$; (iii) $x, -y + {}^3/_2, z + {}^1/_2$; (iv) $'x - 1, -y + {}^3/_2, z + {}^1/_2$. (c) View of the two-dimensional 6^3 net observed for the $(CuI)_\infty$ sheets in **5**.

(23) (a) Healy, P. C.; Pakawatchai, C.; White, A. H. *J. Chem. Soc., Dalton Trans.* **1983**, 1917. (b) Walsdorff, C.; Park, S. O.; Kim, J.; Heo, J.; Park, K. N.; Oh, J.; Kim, K. *J. Chem. Soc., Dalton Trans.* **1999**, 923. (c) Dyason, J. C.; Engelhardt, L. M.; Healy, P. C.; Kildea, J. D.; White, A. H. *Aust. J. Chem.* **1988**, *41*, 335.

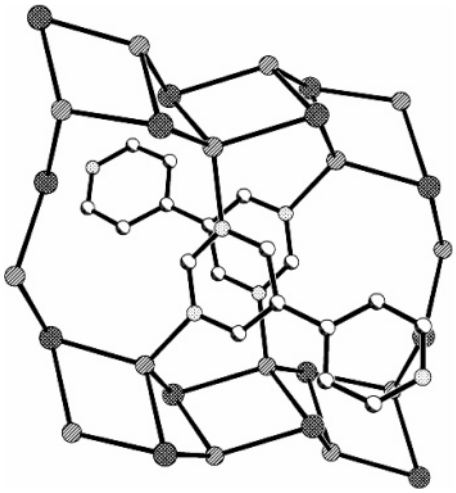

Figure 7. View of the bridging by the pyrimidine group of the pypm ligands across the $(CuI)_\infty$ sheets in compound **5** (Cu, right hatch; N, dotted; I, black, filled circles).

pypm·H_2O is 35(3)°,[24] compared with a corresponding value of 34.0(1)° in **5**. This similarity in dihedral angles between **5** and pypm·H_2O may be purely coincidence or may indicate the possibility that the $(CuI)_\infty$ motif accommodates the preferred ligand conformation.

Conclusions

The angular disposition of the N-donors of the ligands used in this study exerts a defining influence on the oligomeric or polymeric architectures adopted by the CuI complexes. A range of oligomeric and polymeric structures of CuI are observed, the most common being the $(CuI)_2$ rhomboid dimer as in compounds **1** and **3**. Another common motif, $(CuI)_\infty$ chains, is observed in compound **2** which has a strong similarity to a range of compounds observed with linear dipyridyl ligands.[7b] However, the introduction of the combination of different donors, that is, the combination of pyrimidinyl and pyridyl donors in the ligand pypm, leads to a highly unusual $(CuI)_\infty$ sheet structure that combines features of more common chain and stepped cubane $(CuI)_\infty$ motifs.

(24) The two independent molecules in the asymmetric unit of pypm·H_2O exhibit pyrimidine−pyridine dihedral angles of 38.9(1) and 30.7(1)°.

It is clear that controlling CuI structural arrangements remains a significant challenge to those interested in the development of these fascinating structural arrangements and types. The ligand geometry clearly has a significant influence, and the synthesis of certain structural types can be targeted with a degree of success, particularly in two-dimensional sheet structures incorporating $(CuI)_\infty$ chains or ladders with linear dipyridyl ligands,[7b] for example, compound **2**. It is also notable that the use of angular dipyridyl ligands, such as dpt in **1**, dpypy in **3**, and bis(4-pyridyl)disulfide,[7a] favors the formation of $(CuI)_2$ rhomboid dimers.

The introduction of greater structural complexity and variety into the ligands leads to more unusual structural arrangements in the resultant complexes. This may be a result of the $(CuI)_\infty$ oligomer/polymer accommodating the arrangement of donors while providing sufficient donors, in the form of bridging iodide anions, to satisfy the coordination requirements of the copper(I) cations. Thus, a range of structurally unusual complexes have been prepared, including a 2-fold interpenetrated bilayer structure as in **3** and an unexpected $(CuI)_\infty$ sheet structure as in **5**. These framework materials illustrate some of the structural preferences for particular CuI−ligand architectures with greater ligand complexity affording more complex $(CuI)_\infty$ motifs.

Acknowledgment. We thank the Engineering and Physical Sciences Research Council (EPSRC) and the University of Nottingham for funding and the EPSRC National Mass Spectrometry Service Centre in Swansea University for mass spectra. We are grateful to the EPSRC National Crystallography Service at the University of Southampton for data collection on pypm·H_2O. M.S. gratefully acknowledges receipt of a Royal Society Wolfson Merit Award and of a Royal Society Leverhulme Trust Senior Research Fellowship.

Supporting Information Available: Crystallographic data in the form of a CIF file. This material is available free of charge via the Internet at http://pubs.acs.org.

IC052130K